JOURNAL OF VIROLOGY, Apr. 2010, p. 4659–4672 Vol. 84, No. 9
0022-538X/10/$12.00 doi:10.1128/JVI.02725-09

Numerous Conserved and Divergent MicroRNAs Expressed by Herpes Simplex Viruses 1 and 2[▽]

Igor Jurak,[1] Martha F. Kramer,[1] Joseph C. Mellor,[1] Alison L. van Lint,[2]† Frederick P. Roth,[1] David M. Knipe,[2] and Donald M. Coen[1]*

Department of Biological Chemistry and Molecular Pharmacology[1] and Department of Microbiology and Molecular Genetics,[2] Harvard Medical School, Boston, Massachusetts 02115

Received 28 December 2009/Accepted 15 February 2010

Certain viruses use microRNAs (miRNAs) to regulate the expression of their own genes, host genes, or both. Previous studies have identified a limited number of miRNAs expressed by herpes simplex viruses 1 and 2 (HSV-1 and -2), some of which are conserved between these two viruses. To more comprehensively analyze the miRNAs expressed by HSV-1 or HSV-2 during productive and latent infection, we applied a massively parallel sequencing approach. We were able to identify 16 and 17 miRNAs expressed by HSV-1 and HSV-2, respectively, including all previously known species, and a number of previously unidentified virus-encoded miRNAs. The genomic positions of most miRNAs encoded by these two viruses are within or proximal to the latency-associated transcript region. Nine miRNAs are conserved in position and/or sequence, particularly in the seed region, between these two viruses. Interestingly, we did not detect an HSV-2 miRNA homolog of HSV-1 miR-H1, which is highly expressed during productive infection, but we did detect abundant expression of miR-H6, whose seed region is conserved with HSV-1 miR-H1 and might represent a functional analog. We also identified a highly conserved miRNA family arising from the viral origins of replication. In addition, we detected several pairs of complementary miRNAs and we found miRNA-offset RNAs (moRs) arising from the precursors of HSV-1 and HSV-2 miR-H6 and HSV-2 miR-H4. Our results reveal elements of miRNA conservation and divergence that should aid in identifying miRNA functions.

Viruses usurp host mechanisms of gene regulation to control the expression of their own and host genes. For example, a number of viruses, especially the herpesviruses, encode microRNAs (miRNAs), ~22-nucleotide (nt) noncoding RNA molecules that can interfere with the translation and/or stability of target mRNAs (5, 63). miRNA biogenesis begins with the transcription of longer primary transcripts called pri-miRNAs (40). These are then cleaved in the nucleus by the RNase III enzyme Drosha to liberate hairpin structures, usually 60 to 80 nt long, called pre-miRNAs (22, 39). Following export to the cytoplasm, the pre-miRNAs are cleaved further by the RNase III enzyme Dicer to liberate RNA duplexes, which most often are imperfect (18, 29, 38). The RNA duplexes associate with Argonaute (Ago) proteins, Dicer, and GW182 in RNA-induced silencing complexes (RISC), where they are unwound (5, 6, 44, 45). Often, at this stage, one strand (the "star strand") is degraded, while the other strand (mature miRNA) is retained (53). The RISC is guided by the miRNAs to specifically recognize and regulate target mRNAs. In animal mRNAs, miRNA target sites often lie within 3′ untranslated regions (UTRs) (20, 42). Imperfect complementarity of miRNA to the target mRNA most often promotes translational inhibition, as well as some RNA degradation, while perfect complementarity most often promotes RNA degradation (6). When complementarity is imperfect, pairing of miRNA nt 2 to 8, which is known as the seed region, is usually crucial for target recognition and miRNA function (6, 8, 23).

Herpes simplex viruses 1 and 2 (HSV-1 and -2) are members of the *Alphaherpesvirus* subfamily and are important human pathogens, widely known as the causative agents of cold sores and genital herpes, respectively (51). Infections with HSV are usually self-limiting; however, in individuals with immature or compromised immunity, severe morbidity and life-threatening diseases can ensue (51). Typically, the primary site of infection is mucosal epithelium, where the virus enters cells and starts its productive cycle. The productive cycle has been characterized in cell culture and entails a cascade of gene expression (immediate-early, early, and late genes), viral DNA replication, and assembly and egress of infectious virus. In the host, virus can enter sensory neurons that innervate the site of primary infection and establish lifelong latent infection (latency) in which no infectious virus is detected, but from which virus can reactivate and cause recurrent disease. During latency, productive cycle gene expression is repressed, and the most abundant transcripts are the latency-associated transcripts (LATs) (55). The *LAT* locus encodes multiple transcripts, including an unstable 8.3-kb primary transcript and a 2-kb stable intron (17, 19). The exact roles of the LATs are unknown; however, roles in heterochromatin assembly, inhibition of apoptosis, and repression of accumulation of productive-cycle gene products have been ascribed to them (10, 13, 21, 47, 59, 67).

At the time we initiated this study, several HSV-encoded miRNAs had been discovered, all of which are encoded proximal to or within the *LAT* locus (15, 57, 58, 64). The first of these discovered, HSV-1 miR-H1, is expressed relatively abun-

* Corresponding author. Mailing address: Department of Biological Chemistry and Molecular Pharmacology, Harvard Medical School, 250 Longwood Ave., Boston, MA 02115. Phone: (617) 432-1691. Fax: (617) 432-3833. E-mail: Don_Coen@hms.harvard.edu.

† Present address: Australian and New Zealand Intensive Care Society, 10 Ievers Terrace, Melbourne, Victoria, Australia.

▽ Published ahead of print on 24 February 2010.

dantly in productively infected cells as a late gene (15). Five other HSV-1 miRNAs (HSV-1 miR-H2 to miR-H6) were then found to be relatively abundant in latently infected mouse ganglia (64). Three HSV-2 miRNAs, originally designated as HSV-2 miR-I, -II, and -III (57, 58), are positional homologs of HSV-1 miR-H3, -H4, and -H2, respectively, with various degrees of sequence identity. Indeed, HSV-2 miR-III, -I, and -II were recently designated as HSV-2 miR-H2, -H3, and -H4, respectively, by miRBase, the miRNA database (http://www.mirbase.org). We favor that nomenclature, but will also refer to the original terminology. There is limited information on targets of HSV miRNAs. HSV miR-H2, -H3, and -H4 are perfectly complementary to HSV mRNAs encoded on the opposite strands and can downregulate the expression of proteins encoded by these mRNAs (the immediate-early protein, ICP0, for miR-H2, and the late protein, ICP34.5, for miR-H3 and -H4) (58, 64; I. Jurak, S. Lim, P. J. Yen, and D. M. Coen, unpublished data). The seed region of HSV-1 miR-H6 has complementarity with the mRNA encoding the immediate early protein ICP4 and can downregulate its expression (64). Repression of viral transcriptional activators ICP0 and ICP4 by miRNAs may be important for repression of productive-cycle gene expression and thus latency.

We hypothesized that HSV would encode additional miRNAs that had not yet been detected and therefore sought to apply more sophisticated sequencing methods that could increase sensitivity of detection. We chose to examine both productive and latent infection, given that certain HSV miRNAs appear to be more abundant in one setting than another. Finally, we chose to examine both HSV-1 and HSV-2, in part because the eventual identification of targets for mRNAs can be particularly facilitated when miRNAs and their target sequences are evolutionarily conserved (20).

MATERIALS AND METHODS

Cells and viruses. Human embryonic kidney HEK-293 cells (ATCC, CRL-1573) and African green monkey Vero cells (ATCC, CCL-81) were maintained at 37°C in Dulbecco's modified Eagle's medium (Mediatech, Inc.) supplemented with 10% fetal bovine serum or 5% newborn bovine serum, respectively (Sigma-Aldrich). HSV-1 strain KOS (henceforth referred to as HSV-1) and a thymidine kinase (TK)-negative mutant of HSV-2 strain 186syn$^+$,186ΔKpn (30) (henceforth referred to as HSV-2) were propagated and titrated on Vero cells as previously described (14).

Productive and latent infections. For productive infections, HEK-293 cells were infected with HSV-1 or HSV-2 at a multiplicity of infection (MOI) of 5 or 1, respectively, for 18 h. For latent infection, 7-week-old male CD-1 mice (Harlan) were corneally inoculated with 2×10^6 PFU HSV-1 in a volume of 5 μl as previously described (34) or infected intranasally with 1×10^6 PFU of HSV-2 as previously described (30). Trigeminal ganglia were harvested 30 days after infection and immediately frozen as previously described (33).

RNA isolation and sequencing. RNA enriched for small RNA species was extracted from infected cells or trigeminal ganglia using the *mir*Vana kit (Ambion) according to the manufacturer's recommended protocol. For each sample, 10 μg of small-enriched RNA was size fractioned by polyacrylamide gel electrophoresis (PAGE) on a 15% denaturing gel (19:1 acrylamide-Bis solution; Bio-Rad) containing 8 M urea in 0.089 M Tris–0.089 M borate–0.002 M EDTA buffer. RNAs that were 18 to 30 nucleotides were identified by comparison to an SRA ladder (Illumina) and excised from the gel. The gel slices were shredded, and RNA was eluted from the gel for 4 h with 300 μl of 0.3 M NaCl. Gel debris was removed using Spin X cellulose acetate filters (Illumina), and the RNA was precipitated with 1 μl glycogen and 750 μl of 100% ethanol. After being washed with 75% ethanol, the RNA pellet was resuspended in H_2O. Sequencing libraries were created by successive adapter ligation (SRA 5′ and SRA 3′ adapter; Illumina) to the fractioned RNA, followed by cDNA synthesis and amplification by PCR according to the manufacturer's manual (small RNA sample prep kit; Illumina). The libraries were sequenced on the Genome analyzer II (Illumina) at the Biopolymers Facility, Department of Genetics, Harvard Medical School.

Sequencing analysis. The sequences from each library, which consist of 36 nucleotide reads, were first processed with the short oligonucleotide alignment program, SOAP (43), to identify and remove the 5′ flanking sequencing adapter sequence, allowing no mismatches in the adapter. The sequences of the resulting 16 to 26 nucleotide reads from each library were then aligned with SOAP to reference sequences of the HSV-1 strain 17+ genome (NC_001806) or HSV-2 strain HG52 genome (NC_001798), allowing two nucleotide mismatches between sequence reads and the reference genome. Genomic loci represented with three or more sequence reads of ≥19 nucleotides between HSV-1 and HSV-2 in productive or latent infection were then tested by the RNA secondary structure predictions programs mfold and RNAfold (27, 69) for the lowest-free-energy hairpin structures (1). For the hairpin structure analysis, 150 nucleotides of genomic sequence surrounding the locus of the mapped reads was tested.

Northern blots. Vero cells were mock infected or infected with HSV-1 or HSV-2 at an MOI of 10 or 1, respectively. Infected cells were harvested at 18 h postinfection (hpi), and small enriched RNA was prepared as described above. RNA samples, together with a ^{32}P-labeled Decade marker (Ambion), were separated by 15% denaturing PAGE as described above. Gels were soaked briefly in SYBR gold nucleic acid gel stain solution (Molecular Probes). The RNA was then transferred to a BrightStar-Plus positively charged membrane (Ambion) by electroblotting, cross-linked to the membrane using UV light, and prehybridized in ULTRAhyb-Oligo solution (Ambion) for 30 min at 62°C. DNA oligonucleotides (Integrated DNA Technologies) with sequences complementary to miRNAs (see supplemental Table 1 at https://coen.med.harvard.edu) were end labeled with [γ-^{32}P]ATP (MP Biomedicals) and purified using the QIAquick nucleotide removal kit (Qiagen). Overnight hybridizations were performed in ULTRAhyb-Oligo solution (Ambion) at 32°C. Hybridized blots were washed three times briefly and then three times for 15 min in 2× SSC (1× SSC is 0.15 M NaCl plus 0.015 M sodium citrate)–0.5% SDS at 32°C and exposed to a phosphorimager screen. Signals were detected using the Bio-Rad personal molecular imager system. Analyzed blots were stripped using boiling 0.1% SDS solution as previously described (15), exposed to a phosphorimager screen to confirm complete removal of the probe, and successively rehybridized with different probes.

RESULTS AND DISCUSSION

Sequencing analysis. To more completely define the various miRNA species expressed by HSV-1 and HSV-2 during productive and latent infections, we applied massively parallel sequencing of small-RNA libraries using the Illumina Genome Analyzer II. HSV-1 infections were performed with wild-type strain KOS, while HSV-2 infections were performed with 186ΔKpn, a thymidine kinase-negative mutant virus that can establish latent infection in trigeminal ganglia without lethality to mice (30). RNA species of 15 to 30 nt were isolated either from productively infected HEK-293 cells or from latently infected trigeminal ganglia. The RNA was ligated to sequencing adapters, reverse transcribed, and PCR amplified to generate libraries corresponding to small RNA sequences, and sequenced. We acquired between 5×10^5 and 6×10^6 sequence tags from the different samples (see supplemental Table 2 at https://coen.med.harvard.edu). The number of reads for two known cellular miRNAs correlated with the number of all reads obtained in each sample, suggesting that the four sequencing analyses were of similar quality (see supplemental Table 2 at https://coen.med.harvard.edu). Each sequence was 36 nt in length, including adapter sequences, with 13 to 26 nt corresponding to RNA. We limit our analysis here to reads of 19 nt or longer that correspond to sequences within HSV genomes. We were able to assign 6,682 and 856 reads to HSV-1 and 1,6883 and 2,177 reads to HSV-2 from productive and latent infections, respectively (see supplemental Table 2 at https://coen.med.harvard.edu). HSV-specific reads were fur-

ther analyzed manually. A sequence was considered an miRNA candidate when all of three criteria were satisfied. (i, Multiple reads) A particular genomic locus was represented with 3 or more sequencing reads among the four samples. (ii, Hairpin) The sequence was within a hairpin formed by the 150 nucleotides centered on the candidate miRNA and that hairpin was predicted to have lowest free energy by both mfold and RNAfold (1, 27, 69). (iii, Hairpin-loop proximal) When two possible miRNAs were present in the same lowest-energy hairpin, only the one closest to the loop of the hairpin was considered a candidate. Sixty-seven and 363 genomic loci from HSV-1 and HSV-2, respectively (see supplemental Tables 3 and 4 at https://coen.med.harvard.edu), fulfilled criterion 1 and were subsequently tested by mfold and RNAfold. This resulted in selection of 16 and 17 hairpin precursors of miRNAs encoded by HSV-1 and HSV-2, respectively (Tables 1 and 2). All recovered sequence reads of the HSV-1- and HSV-2-encoded miRNAs are listed in supplemental Tables 5 and 6, respectively, at https://coen.med.harvard.edu, and the genomic loci are presented in Fig. 1. When there were different sequences obtained for given miRNAs, the sequences shown in Tables 1 and 2 are the most abundant reads found. We will first summarize the HSV-1 miRNAs, starting with those that have been previously identified, and then discuss the HSV-2 miRNAs, the homologies between HSV-1 and HSV-2 miRNAs, and particular miRNAs of interest.

Previously identified HSV-1 miRNAs. At the time we initiated this study, six HSV-1 miRNAs had been experimentally identified, miR-H1 to miR-H6 (15, 64). As an initial check on our sequencing analysis, we first asked if it identified these 6 miRNAs. Indeed, all 6 were identified, including both mature miRNAs and their corresponding star strands (Tables 1 and 3). Previously, we had not detected star strands for miR-H1, miR-H3, and miR-H5 (15, 64). All of these miRNAs (but not necessarily both strands) were found in both productively and latently infected samples; however, the relative proportions of sequencing reads in the two samples differed considerably. We caution that the relative abundance of sequence reads does not necessarily reflect the relative abundance of one miRNA versus another, as the technique appears to capture certain miRNAs more efficiently than others. However, when the number of reads for one miRNA is greater than the number of reads for a second miRNA in one sample, but lower in another sample, that is likely to reflect differential expression in the two samples. In the HSV-1 productive infection sample, reads for miR-H1 and H6 were the most abundant, whereas in the latent samples they were greatly outnumbered by reads for miR-H2, -H3, and -H4 (Table 1). The analysis also provided the exact sequence of HSV-1 miR-H1, which had previously been detected only by Northern blot hybridization (15). A number of reads corresponding to the original predicted miR-H1 sequence were recovered (see supplemental Table 5 at https://coen.med.harvard.edu). Additionally, reads with mismatches and/or 3′-terminal nontemplated A or U were frequently detected. However, the most abundant miRNA sequence read, which starts 2 nucleotides upstream from the miR-H1 sequence predicted by Cui et al. (15), was selected as HSV-1 miRNA-H1. We will discuss miR-H1 and miR-H6 in more detail in a subsequent section.

Previously predicted HSV-1 miRNAs. Next we asked whether HSV-1 miRNAs whose existence had previously been predicted, but not experimentally verified, were present. Five such miRNAs were found that fulfilled our three criteria, corresponding to predictions by Pfeffer et al. (49), called T-1, T-4, and T-7 by Cui et al. (15), and two predictions by Cui et al. (15), called #6 and #6-RC (Table 1). One of these (T-1) was recently detected in latently infected human ganglia (65) and designated as HSV-1 miR-H8. We designate the other four as HSV-1 miR-H11 (T-4), H12 (#6-RC), H13 (#6) and H14 (T-7). All four of these miRNAs could be detected in productive infection, including both the mature miRNA and the star strand for miR-H14 (Table 1). Among these four, only miR-H8 was also detected in latently infected mouse ganglia (Tables 1 and 3). MiR-H8 is encoded within the second LAT exon, antisense to the first intron of ICP0, consistent with its detection in latently infected ganglia, whereas miR-H14 is encoded within the third exon of *ICP0* mRNA, antisense to miR-H2. Interestingly, miR-H11, -H12, and -H13 are encoded within viral origins of replication (oriL and oriS) and could be derived from previously reported transcripts that span the origins (7, 28, 68). We note that Cui et al. predicted that miR-H13 (#6) would be conserved in HSV-2 (15). We found only one read corresponding to this predicted miRNA from our HSV-1 samples, but found numerous sequencing reads in our sample from HEK-293 cells productively infected with HSV-2, thus fulfilling our multiple-reads criterion; this sequence was also hairpin associated and proximal to the hairpin loop (Tables 1 and 2). We will discuss the origin-encoded miRNAs (miR-H11 to -H13) in more detail below.

Three loci predicted by Cui et al., called #5, #10, and #11, were each recovered as a single sequence read in productively infected samples (see supplemental Table 3 at https://coen.med.harvard.edu); however, these reads fulfilled neither the multiple-reads criterion nor the hairpin criterion and were not designated as HSV-1 miRNAs. The failure of these loci to fulfill the hairpin criterion here, while fulfilling a similar criterion previously (15), might be due to differences in the sequences tested between the two studies. Regardless, we cannot exclude the possibility that the recovered reads are bona fide miRNAs as predicted by Cui et al.

HSV-1 miRNAs that had not been not previously identified or predicted. We also identified 5 additional HSV-1 miRNAs, HSV-1 miR-H7, which has also recently been detected in latently infected human ganglia (65), and miR-H15 to -H18 (Tables 1 and 3). HSV-1 miR-H7, like miR-H8, is encoded within LAT. It is antisense to intron 1 of *ICP0* transcripts. The proportion of HSV-1 miR-H7 reads from latently infected mouse ganglia was higher than that from productively infected HEK-293 cells, which would be consistent with miR-H7 being derived from LAT. HSV-1 miR-H15, which was detected in productively infected cells, is encoded downstream of HSV-1 miR-H6 on the same strand. HSV-1 miR-H16, which was also detected in productively infected cells, is complementary to *UL32* and presumably arises from the 5′ UTR of the transcript encoding *UL33*. Among the HSV-1 miRNAs that we detected, only HSV-1 miR-H11 and -H16 are encoded within unique sequences rather than repeat sequences.

We detected two additional HSV-1 RNAs in both productively and latently infected samples that fulfilled our three

TABLE 1. Predicted hairpin structures of HSV-1 miRNAs

HSV-1 miRNA	Hairpin prediction by mfold[a]	No. of reads/strand[b]	
		Pro	Lat
miR-H1	A-- ACAAC A AA **A AC AA GA** UCC AU 5′GGCG GGA CG GGGG CGGGG**G UGGAAGG GGG GUG** AG UG \ 3′CCGC CCU GC CCCC GCC***UCC ACCUUCC CCC CAC U***C AC A CCA GAGC- - CG ***C GU CC A-*** CU- CC	2555 8	11 -
miR-H2	CGC A - ***G - - A ACU*** UCUU 5′GCCG GCC CC G***UCGCAC CG CCC GGC CAG*** CUGU \ 3′CGGC CGG GG **CAGCGUG GC GGG CCG GUC** GGCG G ACA **- U A A A A C--** CUUG	3 96	5 221
miR-H3	GG G***C UG - A*** UG GU 5′GGGC CCGCGGGCGC ***UCC ACCGCG GGUUCCG GU*** GGC G 3′CCCG GGUGCCCGCG **AGG UGGCGU UCAGGGU** CA UUG G -- **GC GU G C** -- GA	- 67	1 167
miR-H4	U - **A U** G G A 5′GCG GCCGGGG U**GGU GAGUU GACAGGCAAGCA**U UGC UGC G 3′CGC CGGCUC***U AUCG CUCAA CUGUCCGUUC***GUG AUG GCG A **-** ***G - U*** - A G	65 1	130 11
miR-H5	C CCC UC***G CG C*** **-** C UGCC 5′GG GCGU GCGCUCCC ***GGGGGGUU GG AUCUCU AC***CU AG G 3′CC CGCG CGCGGG**GG CCUCCCAA CC UAGAGA UG**GA UC C A CC- **--- A- - C** C UAAC	- 2	2 1
miR-H6	U UCG C- A ***CA U-*** GA- GG 5′GGCGGG GGAC CGGGGGG CGG G***GGUGGAAGG GGGGGGUG A***G UG \ 3′CCGCUC CUUG GCUCCCC GCC **CCUACCUUCC CCCUUCAC** UC AC U **-** UUG UU **C UG** CU AGG UA	83 322	1 3
miR-H7	CUC AG **-** **UGCAA** **-** UCU 5′GGC GGA AGGGGGGAG**AA AGGGGUC CCAAAGG** UGG \ 3′CCG CCU UCUCCCUUCUU UCCCCAG GGUUUCC GCC G C-- CU C CCCUA U UGG	1 -	11 -
miR-H8	C GUCC- **UCA U** CACCC 5′GG GACCCCG CUGUA**UAUAUAGGG GGGGGU CC**G C 3′CC UUGGGGC GAUAUAUAUGUCCC CCCCCG GGU C - ACUGU UGG C ACAAU	2 -	4 -
miR-H11	U 5′GGGCGUGGCCGCUAUUAUAAAAAAAGUGAGAACGCGAAGCGUUCGCACUUUGUCCUAAUAAUA A 3′CCCGCACCGGCGAUAAUAUUUUUUUCACUCUUGCGCUU**CGCAAGCGUGAAACAGGAUU**AUUAU U A	- 7	- -
miR-H12	C C G CC C C AUAU 5′GGAGU GGG ACG CG AGUG UCGCACUUCG CCUAAUA \ 3′CUUCA CUC UGC GC **UCGC AGCGUGAAGC GGGUU**AU A - U - **U- A A** AUAU	- 5	- -
miR-H13	A- C C UAUA 5′GCG AG GUUCGCACUUCGUCC AAUA \ 3′CGC **UC CGAGCGUGAAGCGGG UU**AU U **GG A A** UAUA	- 1	- -
miR-H14	**- *A U U U U*** CGCGAACC 5′GCCGUGUGCC CC ***GUCGCAC CG CCC GGC CAGG***C \ 3′CGGCGCGCGG GG **CAGCGUG GC GGG CCG GUCU**G A U - **C - - U** AGACAAGA	1 3	- -
miR-H15	A- CAUGC G G - C G UUG U 5′ACC CAGCG GCCGG CC UUGUGG GGCCC GG CCGGGGCCCC GG C 3′UGG GUUGC CGGCC GG G**GCACC CCGGG CC GGCCCCGG**GG CC C CG ----- - G **G - G** --- G	- 5	- -
miR-H16	C AG UUA **-** **CA U A---** **AG** CACA 5′GCG AGAG CCUCG AG AG**C GGAGGC GGG UCGA GC** \ 3′CGC UCUC GGGGC UC UCG CUUCCG CCC AGCU CG U U AG CG- G AC C CGCA CG CGCA	8 -	- -
miR-H17	CACU A G G UG G -------| G C 5′GGCC CGC CGCCGCCU CGCGC C G GCC UGGGC CGC G 3′CCGG GCG GU**GGCGGA GCGCG G C CGG** GCCCG GCG C CC-- C **-** **G GU G** UGCAUGU^ - U	- 7	- 2
miR-H18	**A CC ACC**AA GAC C 5′CGGU**CCCGCCCGCCGG CG GGG** CGG GGCGGGCGGCC A 3′GCCAGGGCGGGCGGCC GU CCC GCC CCGCCCGCCGG A G UA CCCC- GUU G	- -	4 -

[a] The ~150-nucleotide sequence surrounding each HSV-1 and HSV-2 miRNA candidate locus was tested by mfold (69), and for each miRNA, the complete hairpin structure of the folding alternative with the lowest free energy is shown. Sequences of mature miRNAs are presented in boldface, and when found in sequencing, the miRNA star strands are shown in boldface and italics.

[b] Numbers represent the number of reads for -5p and -3p strand of each miRNA in the productively (Pro) or latently (Lat) infected sample.

TABLE 2. Predicted hairpin structures of HSV-2 miRNAs

HSV-2 miRNA	Hairpin prediction by mfold[a]	No. of reads/strand[b]	
		Pro	Lat
miR-H2[c]	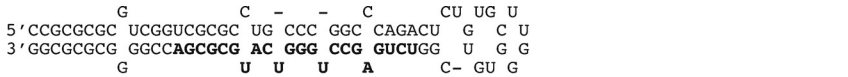	- 15	- 24
miR-H3[c]	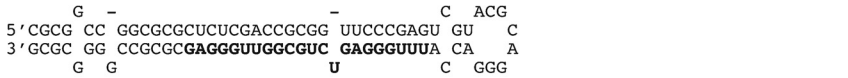	- 352	- 129
miR-H4[c]	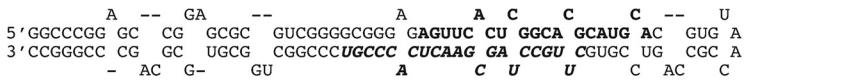	210 85	80 17
miR-H5	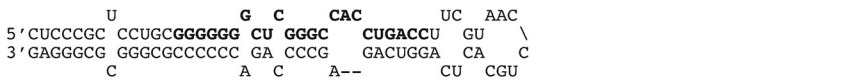	6 -	3 -
miR-H6	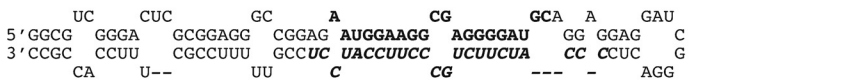	604 2	28 1
miR-H7	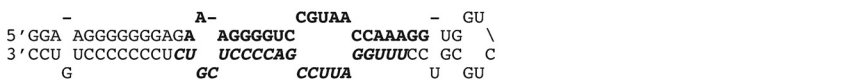	6 3	- -
miR-H9	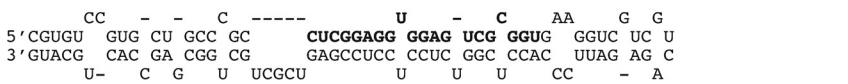	4 -	- -
miR-H11	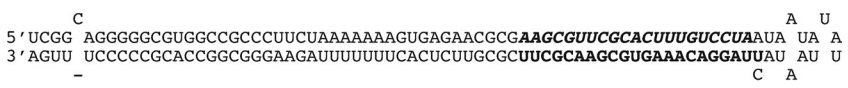	1 73	- -
miR-H12	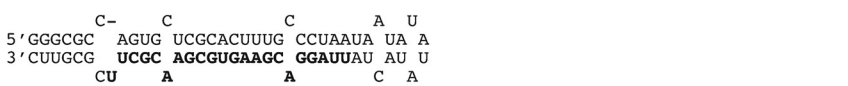	- 29	- -
miR-H13	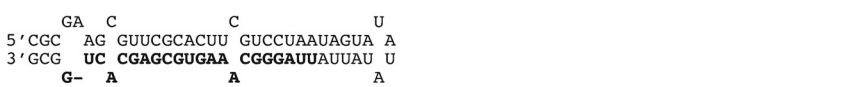	- 50	- -
miR-H19	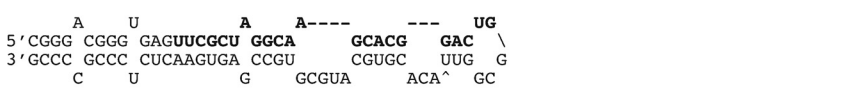	32 -	- -
miR-H20	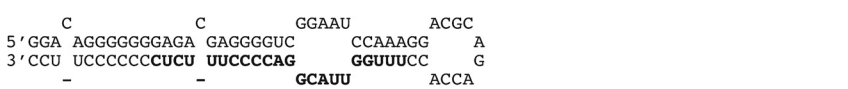	- 27	- -
miR-H21	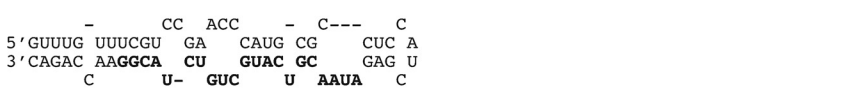	- 12	- -
miR-H22	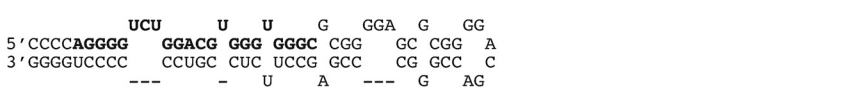	5 -	- -
miR-H23	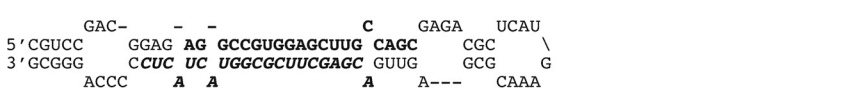	9 9	- -
miR-H24	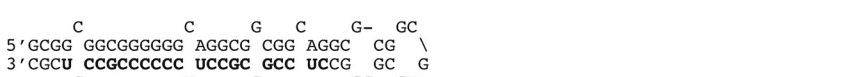	- 20	- 1
miR-H25	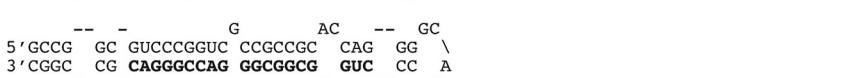	- 10	- -

[a] The ~150-nucleotide sequence surrounding each HSV-1 and HSV-2 miRNA candidate locus was tested by mfold (69), and for each miRNA the complete hairpin structure of the folding alternative with the lowest free energy is shown. Sequences of mature miRNAs are presented in boldface, and when found in sequencing, the miRNA star strands are shown in boldface and italics.

[b] Numbers represent the number of reads for the -5p and -3p strands of each miRNA in the productively (Pro) or latently (Lat) infected sample.

[c] HSV-2 miRNA-H2, miR-H3, and miR-H4 are the miRNA database (www.mirbase.org) designations for miR-III, miR-I, and miR-II, respectively (57, 58).

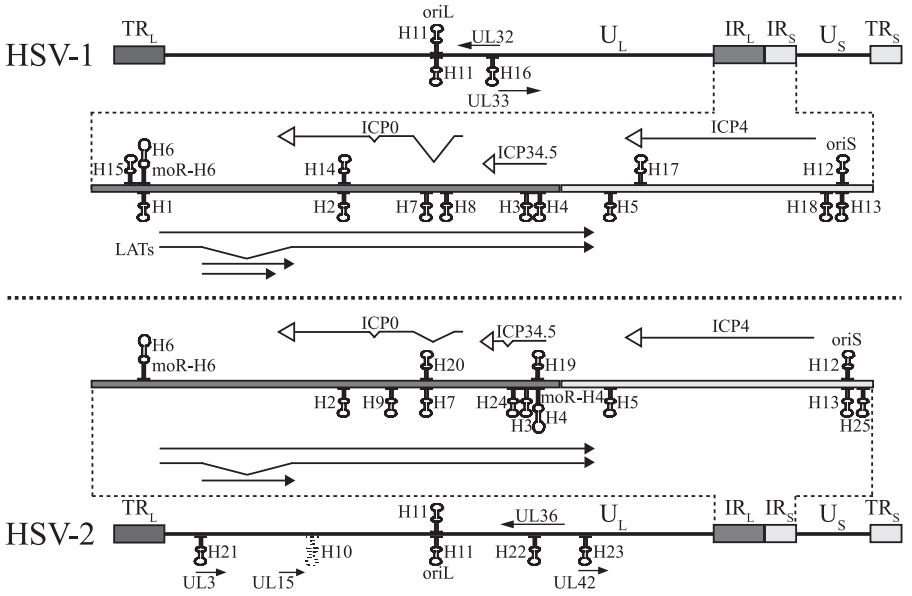

FIG. 1. Genomic location of miRNAs encoded by HSV-1 and HSV-2. The prototype arrangements of the HSV-1 and HSV-2 genomes are depicted at the top and bottom of the figure, respectively. U_L and U_S denote the unique sequences of long (L) and short (S) components of the genome, which are shown as solid lines. Repeat sequences flanking U_L (TR_L and IR_L) and U_S (IR_S and TR_S) are shown as darkly shaded and lightly shaded boxes, respectively. One copy of the internal repeat sequences (IR_L and IR_S) is expanded below and above the HSV-1 and HSV-2 genomes, respectively. Locations and orientations of transcripts in this region are denoted by solid arrows, with angled lines denoting portions removed by splicing. oriL and oriS denote viral origins of DNA replication. The locations of miRNA precursors in the viral genomes are shown as hairpins. miRNA precursors shown below the line are transcribed from left to right (in the same direction as latency-associated transcripts [LATs]), while those above indicate the opposite direction of transcription. In the unique sequences, only transcripts that are encoding, antisense, or close to the pri-miRNAs of the detected miRNAs are shown. The dotted-line hairpin denotes the location of miR-H10, an miRNA detected by Umbach et al. (66) in human ganglia latently infected with HSV-2, but not found in this study.

criteria. One is encoded within ICP4 coding sequences, and thus could arise from *ICP4* mRNA, which has been detected in productively and in latently infected ganglia at low abundance (10, 32, 33, 48). The other is encoded on the opposite strand from *ICP4*, between *ICP4* and oriS, and could arise from anti-4 transcripts, which we have previously detected in latently infected ganglia, and may arise from LAT readthrough transcripts or others (10). We note that these two RNAs are very G-C rich. Nevertheless, there are numerous precedents for G-C-rich miRNAs in the miRNA database (e.g., human miR-762 or miR-718; http://www.mirbase.org). Thus, although our identification of these species as miRNAs is somewhat tentative, we have designated them as HSV-1 miR-H17 (from *ICP4*) and HSV-1 miR-H18 (between *ICP4* and oriS).

HSV-2 miRNAs. (i) miRNAs previously identified. Similar to results from the HSV-1 analysis, we detected all HSV-2 miRNAs that had been identified (57, 58) when we initiated our study (Tables 2 and 3): HSV-2 miR-H2 (originally termed miR-III), HSV-2 miR-H3 (originally termed miR-I), and both strands of HSV-2 miR-H4 (originally termed miR-II-5p and -3p). One of these miRNAs (HSV-2 miR-H4, miR-II) had been predicted computationally prior to its identification (49). These miRNAs were readily detected in both the productive infection and latent infection samples (Table 2). Tang et al. (58) found that HSV-2 miR-H3 (miR-I) was more abundantly expressed in productively infected cells than HSV-2 miR-H2 and miR-H4 (miR-III and miR-II), which is consistent with the relative abundance of sequence reads found in our study. We have extended their results by showing that HSV-2 miR-H2 and miR-H4 (miR-III and miR-II) can also be detected in latently infected mouse ganglia. Recently, Umbach et al. (66) have detected two of these miRNAs (HSV-2 miR-H3/miR-I and HSV-2 miR-H4/miR-II) in human sacral ganglia infected with HSV-2.

(ii) miRNAs previously predicted. We also found sequence reads representing miRNAs that had previously been predicted by Cui et al. (15), Pfeffer et al. (49), or both, but not experimentally verified (Tables 2 and 3). The first of these, which we designate as HSV-2 miR-H5, was detected as the -5p strand in both productive and latent infection, was called #4 by Cui et al. (15), and is homologous to HSV-1 miR-H5. Only the -3p version of HSV-1 miR-H5 was originally detected (64). However, in our current study, we also detected HSV-1 miR-H5-5p in the latently infected sample (Tables 1 and 2). Tang et al. (58) reported that they could not detect either pre-miRNA or mature miRNA species in HSV-2-infected Vero cells using a probe complementary to the -3p strand of an miRNA predicted to be homologous to HSV-1 miR-H5. However, we were able to detect a species corresponding to pre-miRNA in HSV-2-infected Vero and HEK-293 cells using probes complementary to either strand (Fig. 2). In their study, Tang et al. used a different HSV-2 strain, a different procedure for RNA extraction, and also a slightly different probe, which might explain the discrepancy with our results. Although the HSV-1- and HSV-2-specific probes used in the Northern blot analysis were highly similar in sequence, there was no cross-reaction (i.e., the HSV-1 probe did not detect a signal from HSV-2 RNA and vice versa), indicating a highly specific assay (Fig. 2).

TABLE 3. miRNAs expressed by HSV-1 and HSV-2 in productive and latent infections

miRNA	miRNA expression during infection with[a]:				Alternative name	Reference(s)
	HSV-1		HSV-2			
	Productive	Latent	Productive	Latent		
H1	+	+	NH	NH		15, 64
H2	+	+	+	+	HSV-2 miR-III	58, 64–66
H3	+	+	+	+	HSV-2 miR-I	57, 58, 64–66
H4	+	+	+	+	HSV-2 miR-II	57, 58, 64–66
H5	+	+	+	+	#4	15, 64, 65
H6	+	+	+	+		64, 65
H7	+	+	+	+	NN[b]	49, 65, 66
H8	+	+	NH	NH	T-1 (NV)[c]	15, 49, 65
H9	NH	NH	+	−	T-7 (NV)	15, 49, 65, 66
H10	NH	NH	−	−		66
H11	+	−	+	−	T-4 (NV)	15, 49, 65
H12	+	−	+	−	#6RC (NV)	15
H13	+	−	+	−	#6 (NV)	15
H14	+	−	NH	NH		
H15	+	−	NH	NH		
H16	+	−	NH	NH		
H17	+	+	NH	NH		
H18	−	+	NH	NH		
H19	NH	NH	+	−	NN, NV	49
H20	NH	NH	+	−	NN, NV	49
H21	NH	NH	+	−		
H22	NH	NH	+	−		
H23	NH	NH	+	−		
H24	NH	NH	+	+		
H25	NH	NH	+	−		

[a] miRNA was detected (+) or not detected (−) in a productively or latently infected sample. NH, no homolog (HSV-1 or HSV-2 does not encode an miRNA homolog).
[b] NN, not named. miRNA has been predicted, but a specific name has not been designated.
[c] NV, not verified. miRNA has been predicted but not previously experimentally verified.

A second HSV-2 miRNA predicted by Cui et al. was termed #6-RC by those authors (15). This miRNA, as discussed above, arises from a viral origin of replication (oriS), and is homologous to HSV-1 miR-H12. We also detected two HSV-2 miRNAs that had been predicted by Pfeffer et al. (49), which, like HSV-1 miR-H12, are homologous to HSV-1 origin-encoded miRNAs. One of these (prediction termed T-4 by Cui et al. [15]) is encoded within a viral origin of replication (oriL) and is homologous to HSV-1 miR-H11. A second (prediction termed #6 by Cui et al. [15]), which is homologous to HSV-1 miR-H13, is also encoded within a viral origin of replication, in this case, oriS. The three HSV-2 origin-encoded miRNAs (miR-H11 to -H13) were detected only in the productive infection sample and will be discussed in more detail below.

A third miRNA predicted by Pfeffer et al. (49) is homologous to HSV-1 miR-H7, antisense to *ICP0* intron sequences, and could arise from LATs. However, unlike HSV-1 miR-H7, which was readily detected in latent infection (Tables 1 and 3), HSV-2 miR-H7 was detected only in productive infection (Tables 2 and 3). However, the failure to detect this miRNA in the latently infected sample may be due to poor sensitivity. Recently, Umbach et al. detected one read of this miRNA in sacral ganglia samples from one of three latently infected human subjects (66).

There were also two HSV-2 miRNAs predicted by Pfeffer et al. that we have now experimentally verified and for which we have not detected HSV-1 orthologs. Both of these were detected only in the productive infection sample. The first of these, which we designate as HSV-2 miR-H19, arises from the 5′ UTR of the transcript encoding ICP34.5 and is complementary to miR-H4. The second of these, which we designate as HSV-2 miR-H20, is encoded within an *ICP0* intron and is complementary to miR-H7. Of note, we detected one and four reads in HSV-1 productively infected samples that would correspond to homologs of HSV-2 miR-H19 and -H20, respectively. However, these loci did not meet the hairpin criterion and were not regarded as miRNAs.

HSV-2 miRNAs that had not been previously identified or predicted. Of the remaining HSV-2 miRNAs that we detected (Tables 2 and 3), one, which we designate as HSV-2 miR-H6, is a positional homolog of HSV-1 miR-H6, lying upstream of and on the strand opposite to LAT coding sequences. We will discuss this abundantly expressed miRNA in more detail below.

The other newly identified HSV-2 miRNAs, HSV-2 miR-H21 to -H25, are not homologs of HSV-1 miRNAs. HSV-2 miR-H21 to -H23 are encoded within unique long (U_L) sequences and were detected only in the productive infection sample. HSV-2 miR-H21 is encoded within *UL3*, HSV-2 miR-H22 is encoded antisense to coding sequences of *UL36* and might arise from run-through transcripts from the upstream region (*UL30* and *UL33* to *-35* genes), and HSV-2 miR-H23 is encoded within *UL42*. HSV-2 miR-H9, -H24, and -H25 are

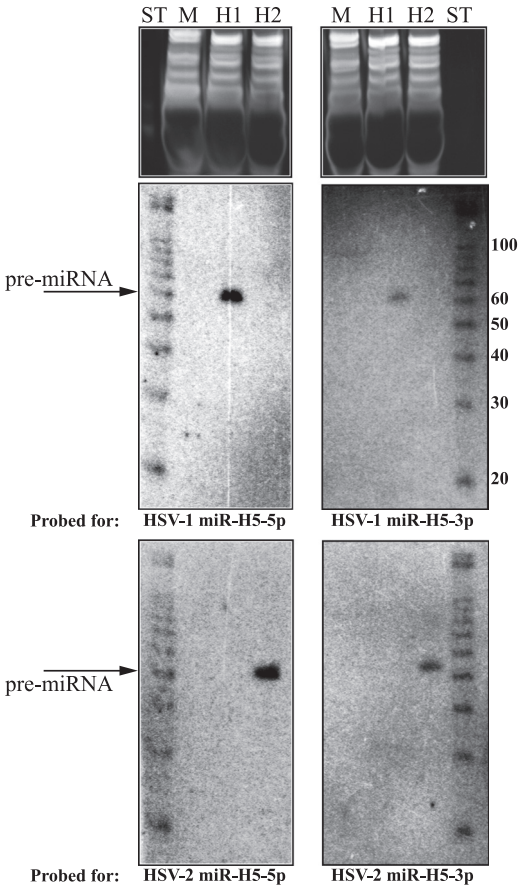

FIG. 2. Northern blot analysis of HSV-1 and 2 miR-H5. Small-enriched RNAs extracted from mock-infected (M) or HSV-1 (H1)- or HSV-2 (H2)-infected HEK-293 cells at 18 h postinfection were resolved by PAGE on two separate gels (left and right panels), stained for tRNAs with SYBR gold (top panels), and blotted to a membrane for hybridization with the probe indicated below each of the middle panels. After the analysis, membranes were stripped and sequentially hybridized with the probes indicated below the bottom panels. The nucleotide sizes of the RNA markers (ST) are indicated to the right of the bottom four panels. The positions of miR-H5 pre-miRNAs are indicated with arrows.

encoded within repeated sequences. HSV-2 miR-H9 and -H24 could arise from LAT sequences, and, indeed, we detected HSV-2 miR-H24 in both productive and latent infection samples. Interestingly, Umbach et al. have recently detected the miR-H9 star strand in three sequence reads from a sacral ganglion sample from one of three subjects infected with HSV-2 (66). HSV-2 miR-H25, which was detected in the productive infection sample, is probably encoded within the same oriS-spanning transcript that encodes miR-H13. The sequence of miR-H25 is very G+C rich, as compared to H13, which may account for the different numbers of recovered reads between H25 and H13. Of note, we did not detect any reads corresponding to an HSV-2 miRNA recently reported by Umbach et al., which they termed HSV-2 miR-H10 (66). This species, which is 85% G+C, is encoded downstream of *UL15* and was found in sequence reads from sacral ganglia from two of three subjects infected with HSV-2. Our failure to detect this RNA could be due to several possible factors. One interesting possibility would be differences in HSV-2 miRNA expression between human sacral ganglia and mouse trigeminal ganglia.

Homologies between HSV-1 and HSV-2 miRNAs. Among the miRNAs that we detected, there are nine positional and/or sequence homologs shared between HSV-1 and HSV-2 (Table 4). Of these nine miRNAs, we found both -5p and -3p strands from both viruses for two. It is interesting to compare the sequences of these orthologs, particularly conservation of the seed region, a major determinant of miRNA function. We first asked what fraction of the seven bases in the seed region were identical between orthologs; a high fraction of identity strongly suggests conserved targets for the orthologous miRNAs. However, even when sequences are not identical between orthologs, when the differences in sequence are G:A or C:U, it is possible that these miRNAs still recognize the same mRNA targets (i.e., by G-U and A-U pairing and C-G and U-G pairing). Therefore, we also assessed "seed consistency" (41, 42), the fraction of bases in the seed region of orthologous miRNAs that can retain their ability to base pair with a common target sequence (Table 4). We note that for some miRNAs, the sequence reads differ at their ends, and for the conservation analysis, we used the most abundantly found reads between productive and latent infection (Table 4).

Tang et al. (58) described HSV-1 and HSV-2 miR-H2 (HSV-2 miR-III) as having minimal sequence similarity. Our analysis shows that they share 72% identity overall and completely identical seed regions. This raises the possibility that the miR-H2 orthologs not only can repress expression of ICP0, to whose mRNA they are completely complementary, but that they may repress the expression of other conserved targets as well.

As noted by Tang et al. (57, 58), comparison of the miR-H3 and miR-H4 orthologs of HSV-1 and HSV-2 reveals incomplete sequence identity in the seed region (Table 4). This can be interpreted (57, 58) as implying that these miRNAs are unlikely to have conserved targets other than ICP34.5, whose mRNA is complementary to these miRNAs. However, the miR-H4-3p orthologs exhibit 6/7 seed identity and 7/7 seed consistency, and the miR-H3-3p orthologs exhibit 5/7 seed identity and 6/7 seed consistency. Thus, these orthologs might have conserved targets other than ICP34.5.

Similarly, HSV-2 miR-H5 shares 74% overall sequence identity with HSV-1 miR-H5, including six of seven bases in the seed region and 7/7 seed consistency (Table 4), which might suggest conserved targets. Of the remaining orthologs, all but one (miR-H6; see below) show considerable seed identity ($\geq$6/7 identity), and all show maximal seed consistency (7/7), again suggesting conserved targets for these orthologs.

The miR-H5 orthologs, which are expressed in latent infection, are not completely complementary to any known viral transcript. Their well-conserved seed regions are very G rich. Perhaps they interact with mRNAs with homopolymeric runs of C, of which there are several HSV examples (12, 46), or, given the unusual structures that runs of G's can form, perhaps they function using interactions other than Watson-Crick base pairing. The miR-H7 orthologs are also expressed in latency (66; this report). These miRNAs are highly homologous (86% identical with 7/7 identity in the seed region). Interestingly, they are antisense to *ICP0* first intron sequences and, as pointed out by Umbach et al. (66), are therefore unlikely to downregulate ICP0 expression. We have previously described

TABLE 4. miRNA homologs expressed by HSV-1 and HSV-2

HSV-1 and HSV-2 miRNA homolog	miRNA sequence[a]	No. of identical nt/total in seed region (nt positions 2–8)		Location	Proposed target (reference)
		Identity[b]	Consistency[c]		
miR-H2-3p HSV-1 HSV-2	C**CUGAGCC**AGGGACGAGUGCGACU U**CUGAGCC**UGGGUCAUGCGCGA-- †******* *** *† *†****	7/7	7/7	Within 2nd Lat exon; complementary to ICP0 3rd exon	ICP0 (58, 64)
miR-H3-3p HSV-1 HSV-2	-C**UGGGACU**GUGCGGUUGGGAC U**UUGGGAG**UCUGCGGUUGGGAG †***** * **********	5/7[d]	6/7[d]	Within 2nd LAT exon and L/STs; complementary to ICP34.5 ORF	ICP34.5 (57)
miR-H4-5p HSV-1 HSV-2	G**GUAGAGU**UUGACAGGCAAGCA A**GUUCA-CU**CGGCACGCAUGCA †** * †* *†** *** ***	4/7	5/7	Within 2nd LAT exon and L/STs; complementary to ICP34.5 5'UTR	ICP34.5 (58)
miR-H4-3p HSV-1 HSV-2	C**UUGCCUG**UCUAACUCGCUAGU C**UUGCCUA**GCGAACUCACCCGU *******† * *****†*† **	6/7	7/7		
miR-H5-5p HSV-1 HSV-2	G**GGGGGGU**UCGGGCAUCUCUACC G**GGGGGGC**UCGGGCCACCUGACC *******†****** *†† ***	6/7	7/7	Within 2nd LAT exon and L/STs	Unknown
miR-H6-5p HSV-1 HSV-2	G**GUGGAAG**GCAGGGGGGUGUA A**AUGGAAG**GCGAGGGGAUGC- ††*********††*****†**	6/7	7/7	Opposite strand and upstream of LATs; complementary to HSV-1 miR-H1	Unknown
miR-H6-3p HSV-1 HSV-2	--C**ACUUCCC**GUCCUUCCAUCCC C**CCAUCUU**CUGCCCUUCCAUCCU **†††*†*†*†**********	3/7[d]	7/7		ICP4 (64)
miR-H7-5p HSV-1 HSV-2	A**AAGGGGU**CUGCAACCAAAGG A**AAGGGGU**CCGUAACCAAAGG *********†*†**********	7/7	7/7	Within 2nd Lat exon; complementary to ICP0 1st intron	Unknown
miR-H11-3p HSV-1 HSV-2	U**UAGGACA**AAGUGCGAACGC-- U**UAGGACA**AAGUGCGAACGCUU ********************	7/7	7/7	oriL	Unknown
miR-H12-3p HSV-1 HSV-2	U**UGGGACG**AAGUGCGAACGCUU U**UAGGACG**AAGUGCGAACGCUU **†********************	6/7	7/7	oriS	Unknown
miR-H13-3p HSV-1 HSV-2	U**UAGGGCG**AAGUGCGAGCACUGG U**UAGGGCA**AAGUGCGAGCACUG- *******†***************	6/7	7/7	oriS	Unknown

[a] Sequences of orthologous miRNAs expressed by HSV-1 (top sequence) and HSV-2 (bottom sequence) aligned using ClustalW2 (37). The seed sequences are shown in boldface. Identical nucleotides and nucleotides with conserved target binding potential are indicated with * and †, respectively.

[b] The numerator is the number of identical nucleotides in the seven-nucleotide (nt 2 to 8) seed region, and the denominator is the number of total nucleotides (always 7) in the seed region.

[c] The numerator is the number of nucleotides in the seed region with conserved target binding potential (based on G:U base pairing), and the denominator is the number of total nucleotides (always 7) in the seed region.

[d] Maximum score for sequence identity or consistency when alignment resulted in gaps affecting the seed region.

ICP0 transcripts that contain the first intron in latently infected ganglia (11), which may be related to similar transcripts found in productively infected cells (9). However, mutations that drastically reduce LAT expression, and would therefore be expected to drastically reduce miR-H7 expression, did not result in an increase in the levels of these intron-containing transcripts (11), as would be expected if miR-H7 downregulates their expression at the transcript level. Thus, especially given the high identity of the seed region of the two orthologs, we favor miR-H7 having other conserved targets, either viral, cellular, or both.

The miR-H1/miR-H6 locus. The miRH1/6 locus lies about 300 bp upstream of the *LAT* transcription start site. In HSV-1, miR-H1 and miR-H6 are derived from hairpins that are encoded on opposite strands (Fig. 1 and 3). As noted above, the most abundant sequence reads in the HSV-1 productive infection sample were for HSV-1 miR-H1-5p, consistent with its ready detection by Northern blot hybridization (15). Interestingly, we found 11 reads of HSV-1 miR-H1-5p in the latent infection sample. We had not previously detected this miRNA in latently infected material using 454 sequencing or stem-loop reverse transcription-PCR (RT-PCR). However, the former method generates fewer sequence reads than the Illumina sequencing technology used here, and the RT-PCR assay for this miRNA has a high background (64; M. F. Kramer, I. Jurak, and D. M. Coen, unpublished data). Thus, it is possible that HSV-1 miR-H1 is an authentic latent transcript, expressed consistently in latently infected ganglia. It is also possible that this miRNA is expressed less consistently at low levels, like a number of other productive cycle transcripts (10, 11, 16, 32, 33,

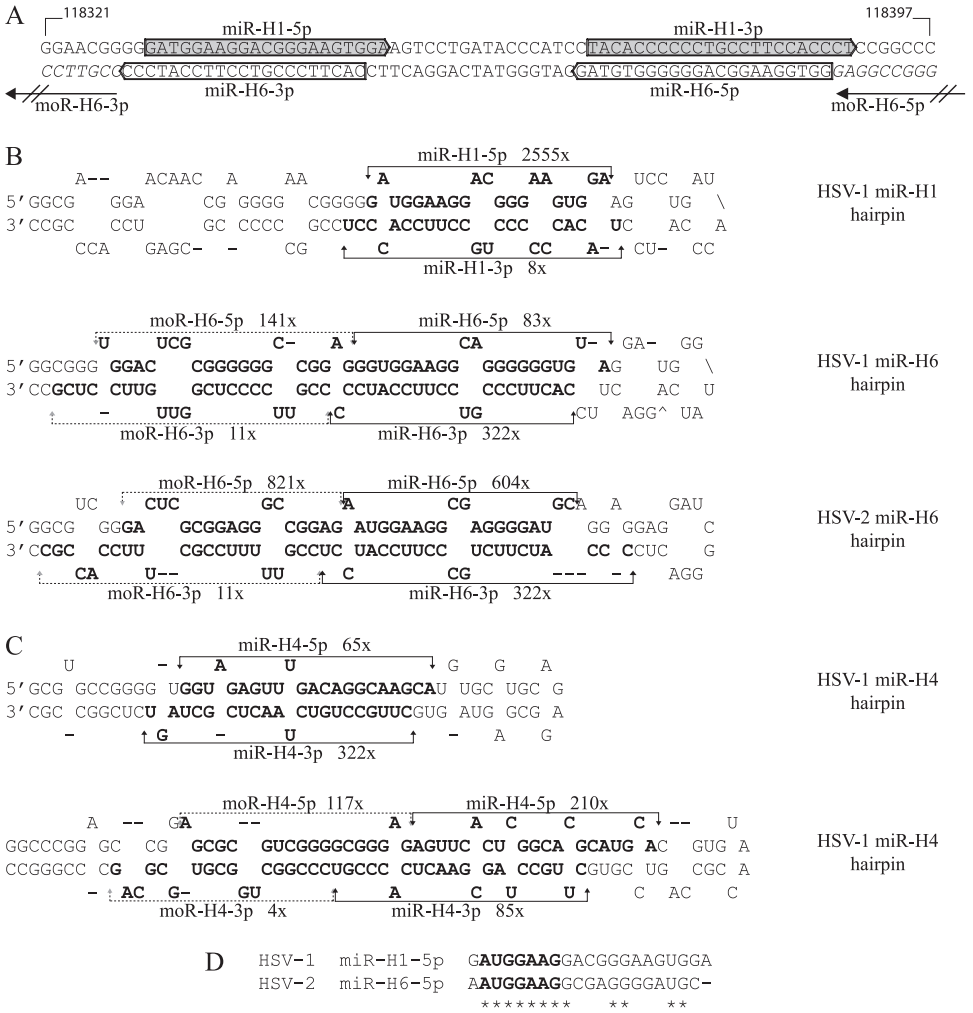

FIG. 3. miRNA H6 and H4 loci. (A) Sequence of the genomic locus encoding complementary miRNAs, HSV-1 miR-H1 and -H6. The boxes indicate -3p and -5p strands of miR-H1 (gray shading) and miR-H6 (no shading), with arrows indicating the direction of transcription. Parts of the sequences encoding moR-H6-5p and -3p are shown in italics, with discontinued arrows indicating the direction of transcription. Nucleotide coordinates for the IR_L copy of the locus according to HSV-1 strain 17+ genome (NC_001806) are shown on the top of the panel. (B and C) Hairpin structures of HSV-1-encoded precursor of miR-H1 and miR-H6 and HSV-2-encoded precursor of miR-H6 (B); and hairpin structures of HSV-1- and HSV-2-encoded precursors of miR-H4 (C). The most prominently found sequence reads are shown in boldface and encompassed by brackets with arrows. Solid or dotted lines indicate miRNA or moR sequences, respectively. Black and gray arrows point to Dicer and presumed Drosha cleavage sites, respectively. The numbers of detected sequence reads in the productive infection sample are shown below and above the corresponding miRNA or moR strand. (D) Sequence comparison of HSV-1 miR-H1-5p and HSV-2 miR-H6-5p. The seed sequence of each miRNA is shown in boldface, and the identical nucleotides are indicated with the asterisks.

48, 56). Resolving this question will require further investigation. Interestingly, we did not detect a positional homolog of HSV-1 miR-H1 in either the HSV-2 productive or latent infection sample (but see below).

The second most abundant sequence reads in the HSV-1 productive infection sample were for HSV-1 miR-H6-3p. HSV-1 miR-H6-5p had substantially fewer reads. In contrast, the most abundant sequence reads in the HSV-2 productive infection sample were for HSV-2 miR-H6-5p, with very few reads for HSV-2 miR-H6-3p. Consistent with the abundant sequence reads in the productive infection samples, we could readily detect the pre-miRNA and mature forms of HSV-1 and HSV-2 miR-H6 in RNA from productively infected Vero and 293 cells using Northern blot hybridization, probing for the strands that were more abundant in the sequence reads (Fig. 4). We also detected HSV-1 miR-H6-3p in the latent infection sample, consistent with its previous detection in latently infected mouse and human trigeminal ganglia (64, 65). We also found one read of HSV-1 miR-H6-5p in the latent sample. For HSV-2, we detected miR-H6-5p in 28 reads from the latent sample and one read of miR-H6-3p.

It is interesting to compare the sequences of the different miRNAs from the miR-H1/miR-H6 locus (Fig. 3). HSV-1 miR-H6-5p and HSV-2 miR-H6-5p are 74% identical, with 6/7 seed identity and 7/7 seed consistency (Table 4), suggesting functional conservation. In contrast, although HSV-1 miR-H6-3p and HSV-2 miR-H6-3p share considerable sequence identity, most of that is in their 3′ ends, with very little seed identity (Table 4). This raises questions regarding whether miR-H6-3p exhibits functional conservation, especially as

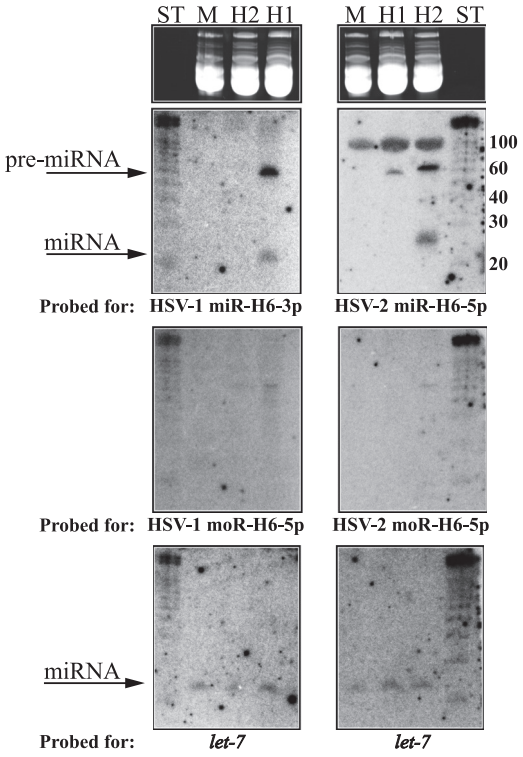

FIG. 4. Northern blot analysis of HSV-1 and -2 miR-H6 and moRs. Small-enriched RNAs extracted from mock-infected (M) or HSV-1 (H1)- or HSV-2 (H2)-infected HEK-293 cells at 18 h after infection were resolved by PAGE on two separate gels (left and right panels), stained for tRNAs with SYBR gold (top panels), and blotted to a membrane for hybridization with the probe indicated below the next panel below. After analysis, membranes were sequentially stripped and hybridized with the probes indicated below the next panel down. The positions of pre-miR-H6, miR-H6, and cellular miRNA let-7 are indicated with arrows. The nucleotide sizes of the RNA markers (ST) are indicated to the right of the panels.

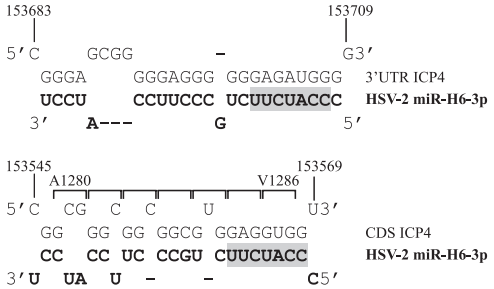

FIG. 5. Complementarity of HSV-2 miR-H6 with *ICP4* mRNA. (A) Predicted complementarity between HSV-2-encoded miR-H6-3p and a sequence in the HSV-2 *ICP4* 3′ untranslated region (3′ UTR) (top) and a coding sequence (CDS) (bottom), predicted using RNAhybrid (35, 50). Nucleotide coordinates for the *ICP4* region complementary to miR-H6 based on the HSV-2 strain HG52 genome (NC_001798) are shown on the top of each panel. The seed sequences of miRNAs are highlighted by gray shading. The ICP4 CDS corresponds to amino acids A1280 to V1286 of HSV-2 ICP4, as indicated at the top of the bottom panel.

HSV-1 miR-H6-3p exhibits seed complementarity with HSV-1 *ICP4* mRNA and can translationally repress HSV-1 ICP4 expression (64). However, despite the lack of seed identity between the miR-H6-3p orthologs, HSV-2 miR-H6-3p exhibits considerable complementarity, including complete seed complementarity with sequences in the 3′ UTR and coding region of HSV-2 *ICP4* mRNA (Fig. 5). Moreover, the two miR-H6-3p orthologs exhibit high seed consistency (7/7; Table 4), consistent with the possibility of conserved function.

Perhaps most intriguingly, two miRNAs that are highly abundant during productive infection, HSV-1 miR-H1-5p and HSV-2 miR-H6-5p, exhibit complete seed identity, despite <60% overall sequence identity (Fig. 3D). This suggests that these miRNAs function to downregulate similar targets during infection. It will be interesting to determine the targets of the various miRNAs expressed from this locus, especially as these miRNAs are both highly abundant in productive infection and can be detected in latently infected ganglia.

HSV-encoded moRs. Unexpectedly, we detected abundant sequence reads for ~22-nt RNAs that arise from the same hairpin that is predicted for miR-H6. These miRNAs are encoded immediately adjacent to the two strands of miR-H6, distal to the loop of the hairpin (Fig. 3B). However, despite showing similar abundance in the sequence reads to miR-H6, and despite our being readily able to detect miR-H6 by Northern blot hybridization, we were unable to detect these RNAs by the same method (Fig. 4). Similarly, we observed small RNAs with the same properties arising from the HSV-2 miR-H4 (miR-II) locus (Fig. 3C), but not the HSV-1 miR-H4 locus. These RNAs did not fulfill our hairpin-loop proximal criterion for miRNAs; thus, we are reluctant to designate them as miRNAs. Rather, we designate these RNAs as miRNA-offset RNAs (moRs), a term that has been applied to small RNAs detected in the simple chordate *Ciona intestinalis*. There have recently been reported moRs in *Drosophila melanogaster*, mouse embryonic stem cells, and humans, albeit at very low expression levels (2, 36, 52, 54). Moreover, Umbach et al. detected moRs derived from pri-miRNAs encoded by Kaposi's sarcoma-associated herpesvirus (KSHV) in a latently infected cell line (62). The biogenesis of this new class of small RNA molecules is poorly understood; however, it has been proposed that moRs might arise from Drosha processing of pri-miRNAs rather than successive Dicer processing of one long pre-miRNA (54). Our Northern blot analysis of moR-H6 is consistent with the Drosha biogenesis model, as we could not detect pre-miRNA using the moR antisense probe (Fig. 4). Further investigation will be required to understand the expression and actual abundance of these RNAs.

A family of origin-encoded miRNAs. As described above, both HSV-1 and HSV-2 express miRNAs that are encoded within origins of replication: miR-H11, encoded within oriL, and miR-H12 and miR-H13, encoded within oriS. The sequences of these miRNAs and their locations relative to origin sequences are shown in Fig. 6. Notably, the HSV-1 oriL hairpin, being a 144-bp perfect palindrome, does not have any internal mismatch bulges that are typically found in pri-miRNAs or pre-miRNAs (1), and the HSV-2 hairpin has only 1 single nucleotide mismatch (Tables 1 and 2). MiR-H11 lies entirely within oriL (Fig. 6). Thus, there are two copies of miR-H11 coding sequences; whether both are expressed is not clear. In contrast, miR-H12 and miR-H13 are encoded from opposite strands and extend outside the oriS palindromes, so

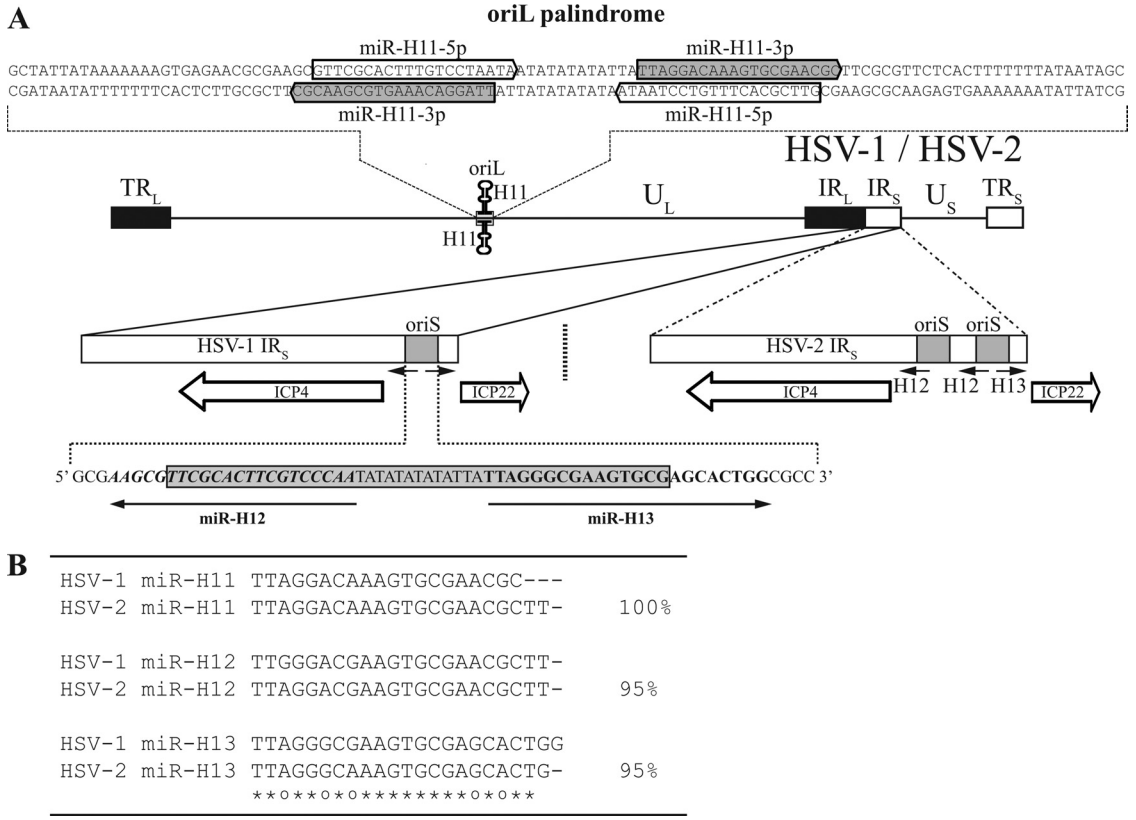

FIG. 6. Family of miRNAs arising from the origins of replication. (A) In the middle of the panel is shown a schematic view of the HSV-1 and HSV-2 genomes. U_L and U_S denote the unique sequences of long (L) and short (S) components, respectively, of the genome, which are shown as solid lines. Repeat sequences flanking U_L (TR_L and IR_L) and U_S (IR_S and TR_S) are shown as filled and unfilled boxes, respectively. Below are shown expanded views of the HSV-1 (left, connected with a solid line) and HSV-2 (right, connected with a dotted line) IR_S regions. Viral origins of DNA replication, oriL and oriS, are shown as gray boxes. Locations of miRNAs miR-H12 (H12) and miR-H13 (H13) and *ICP4* and *ICP22* transcripts are shown, with arrows indicating the direction of transcription. At the bottom of the panel to the left is shown the sequence of HSV-1 oriS (shaded box), the sequences of HSV-1 miR-H12 and miR-H13 are shown in boldface, and the direction of transcription is indicated with arrows. At the top of the panel is shown the sequence of HSV-1 oriL. HSV-1 miR-H11-3p and the predicted -5p star strand are shown as shaded boxes outlined with solid and dotted lines, respectively. (B) Sequence comparison of the origin of replication family miRNAs (miR-H11, -H12, and -H13) encoded by HSV-1 and HSV-2. The numbers indicate percentage of sequence identity between two orthologous miRNAs. Identical nucleotides and nucleotides with conserved target binding potential (consistency) are indicated with asterisks and small circles, respectively.

that the two miRNAs have 5′ ends in common but divergent 3′ ends. Adding further complexity, HSV-2 contains 2 copies of oriS in each short repeat (R_S) (Fig. 6A). These two oriS palindromes are surrounded by highly similar, but nevertheless distinctive sequences, and since miR-H13 extends outside of oriS, it is possible to distinguish, not just the orientation, but also the exact oriS copy from which this miRNA arises (Fig. 6A). Notably, miR-H11 to -H13 share considerable sequence identity throughout, both within each virus species and between species (Fig. 6B). In particular, the seed regions show 7/7 consistency and are identical for three of the six miRNAs (both miR-H11 and HSV-2 miR-H13), differing by only one base for two (HSV-2 miR-H12 and HSV-1 miR-H13) and only two bases for the remaining one (HSV-1 miR-H12) (Table 4 and Fig. 6B). Thus, these miRNAs constitute a family and may have common targets.

In HSV-1, the DNA sequences encoding HSV-1 miR-H11 include sites for binding by the origin-binding protein, UL9, and also glucocorticoid-response element half-sites (25, 26). In mice following corneal inoculation, a double-point mutant that would affect both coding sequences for miR-H11 exhibited modestly decreased acute replication and reactivation from latency accompanied by reduced pathology and mortality (4). Although there is considerable reason to think that these phenotypes in mice are due to effects of the mutations on DNA replication (3, 4, 26), we raise the possibility that one or more of the phenotypes may be due to loss of the function of miR-H11.

Complementary miRNAs. As described previously (64), HSV-1 encodes two miRNAs encoded on complementary strands: miR-H1 and miR-H6. Our analysis has identified several other such pairs. These are HSV-1 miR-H2 and miR-H14, HSV-2 miR-H4 and miR-H19, and HSV-2 miR-H7 and miR-H20 (Fig. 1). All complementary pairs are transcribed from palindrome-like sequences, and each miRNA pair shares substantial sequence identity, which suggests that they might target conserved mRNAs, as has been recently proposed for some *D. melanogaster* antisense miRNA pairs (61). An additional intriguing possibility is that each miRNA in the pair might have a role in repression of the transcripts encoding the complementary miRNA or might even block the functions of the mature complementary miRNA.

miRNAs and latency. The miRNAs that we have detected are encoded disproportionately within the repeat sequences of the HSV genome (Fig. 1). We do not think it is an accident that this is also the region that is transcriptionally most active during latency. Indeed, only a handful of HSV-1 miRNAs were not detected in the latent infection sample; these were the two unique long region (U_L)-derived miRNAs, the two oriS-derived miRNAs miR-H14 (which is encoded within *ICP0*), and miR-H15 (which is encoded on the same strand as and downstream of miR-H6). Perhaps more telling, all of the HSV-1 miRNAs that had more abundant reads in the latent infection sample than in the productive infection sample and all but one of the HSV-2 miRNAs that were detected in the latent infection sample are encoded on the same strand as LATs and are downstream of the *LAT* promoter. It will be particularly interesting to identify promoters that drive expression of miRNAs such as miR-H6 that are encoded from the opposite strand from LATs.

Have we identified the complete set of miRNAs expressed by HSV-1 and HSV-2? In this study, we have confirmed and extended previous identifications of HSV miRNAs (15, 57, 58, 64, 65), so that 16 HSV-1 miRNAs and 17 HSV-2 miRNAs are now known. Do we now know the entire complement of HSV miRNAs? There are several grounds to suggest that we do not. First, only one HSV-1 and one HSV-2 strain are completely sequenced and available. Small sequence differences between the strains with which we worked and these sequenced strains might have excluded certain hairpins and thus certain loci from further analysis. In fact, we have identified numerous loci with a high number of sequence reads that did not pass the hairpin criterion. Second, different strains might express strain-specific miRNAs, which might account for differences in pathogenicity. Thus, it would be particularly interesting to compare clinical isolates with laboratory strains. Third, in our analysis we did not detect a single sequence read for HSV-2 miR-H10 (UL15) detected by Umbach et al. (66) from latently infected human ganglia. We cannot exclude the possibility that this miRNAs is strain specific or that it is only expressed in the human host. Along these lines, our productive infection samples were all harvested at a rather late time point. We cannot exclude the possibility of miRNAs that are more abundant earlier in infection. In other words, experimental settings might account for important differences in analyses. Finally, the development of new technologies and bioinformatic tools might increase the sensitivity of detection, leading to the discovery of additional HSV miRNAs.

Roles of miRNAs. A key question is what are the roles of the HSV miRNAs that have been identified? For some previously identified miRNAs (i.e., miR-H2 to -H4), identification of viral targets has been facilitated by the fact that these miRNAs are transcribed from the opposite strand of known viral mRNAs, which makes them obvious targets (57, 58, 64, 65). However, for most miRNAs there is no obvious target. The challenge will be to identify them. Moreover, the functions of these miRNAs might not be limited just to RISC-dependent posttranscriptional regulation, but might also include transcriptional regulation (31) and direct effects on the stability of mRNAs that contain hairpins from which miRNAs, in principle, could be derived (24, 60). Regardless, the ability to compare miRNAs from HSV-1 and HSV-2 should greatly aid efforts to identify HSV miRNA functions.

ACKNOWLEDGMENTS

We thank the West Quad Computing Group at Harvard Medical School for computational resources and support. We gratefully thank Bryan Cullen and Jennifer Umbach for communicating results prior to publication. We also gratefully acknowledge the assistance received from all members of the Coen laboratory and, in particular, valuable discussions with Jeremy Kamil and Blair Strang.

This work was supported by NIH grants RO1 AI26126 (to D.M.C.) and PO1 NS35138 (to D.M.C. and D.M.K.), H600423, H6004756, H6003224, and H60017115 and by the Canadian Institute for Advanced Research (to F.P.R.). J.C.M. was supported by an Individual NRSA from NIH/NHGRI (H6004825).

REFERENCES

1. **Ambros, V., B. Bartel, D. P. Bartel, C. B. Burge, J. C. Carrington, X. Chen, G. Dreyfuss, S. R. Eddy, S. Griffiths-Jones, M. Marshall, M. Matzke, G. Ruvkun, and T. Tuschl.** 2003. A uniform system for microRNA annotation. RNA **9:**277–279.
2. **Babiarz, J. E., J. G. Ruby, Y. Wang, D. P. Bartel, and R. Blelloch.** 2008. Mouse ES cells express endogenous shRNAs, siRNAs, and other Microprocessor-independent, Dicer-dependent small RNAs. Genes Dev. **22:**2773–2785.
3. **Balliet, J. W., J. C. Min, M. S. Cabatingan, and P. A. Schaffer.** 2005. Site-directed mutagenesis of large DNA palindromes: construction and in vitro characterization of herpes simplex virus type 1 mutants containing point mutations that eliminate the oriL or oriS initiation function. J. Virol. **79:** 12783–12797.
4. **Balliet, J. W., and P. A. Schaffer.** 2006. Point mutations in herpes simplex virus type 1 oriL, but not in oriS, reduce pathogenesis during acute infection of mice and impair reactivation from latency. J. Virol. **80:**440–450.
5. **Bartel, D. P.** 2004. MicroRNAs: genomics, biogenesis, mechanism, and function. Cell **116:**281–297.
6. **Bartel, D. P.** 2009. MicroRNAs: target recognition and regulatory functions. Cell **136:**215–233.
7. **Bludau, H., and U. K. Freese.** 1991. Analysis of the HSV-1 strain 17 DNA polymerase gene reveals the expression of four different classes of pol transcripts. Virology **183:**505–518.
8. **Brennecke, J., A. Stark, R. B. Russell, and S. M. Cohen.** 2005. Principles of microRNA-target recognition. PLoS Biol. **3:**e85.
9. **Carter, K. L., and B. Roizman.** 1996. Alternatively spliced mRNAs predicted to yield frame-shift proteins and stable intron 1 RNAs of the herpes simplex virus 1 regulatory gene alpha 0 accumulate in the cytoplasm of infected cells. Proc. Natl. Acad. Sci. U. S. A. **93:**12535–12540.
10. **Chen, S. H., M. F. Kramer, P. A. Schaffer, and D. M. Coen.** 1997. A viral function represses accumulation of transcripts from productive-cycle genes in mouse ganglia latently infected with herpes simplex virus. J. Virol. **71:** 5878–5884.
11. **Chen, S. H., L. Y. Lee, D. A. Garber, P. A. Schaffer, D. M. Knipe, and D. M. Coen.** 2002. Neither LAT nor open reading frame P mutations increase expression of spliced or intron-containing ICP0 transcripts in mouse ganglia latently infected with herpes simplex virus. J. Virol. **76:**4764–4772.
12. **Chou, J., and B. Roizman.** 1990. The herpes simplex virus 1 gene for ICP34.5, which maps in inverted repeats, is conserved in several limited-passage isolates but not in strain 17syn+. J. Virol. **64:**1014–1020.
13. **Cliffe, A. R., D. A. Garber, and D. M. Knipe.** 2009. Transcription of the herpes simplex virus latency-associated transcript promotes the formation of facultative heterochromatin on lytic promoters. J. Virol. **83:**8182–8190.
14. **Coen, D. M., H. E. Fleming, Jr., L. K. Leslie, and M. J. Retondo.** 1985. Sensitivity of arabinosyladenine-resistant mutants of herpes simplex virus to other antiviral drugs and mapping of drug hypersensitivity mutations to the DNA polymerase locus. J. Virol. **53:**477–488.
15. **Cui, C., A. Griffiths, G. Li, L. M. Silva, M. F. Kramer, T. Gaasterland, X. J. Wang, and D. M. Coen.** 2006. Prediction and identification of herpes simplex virus 1-encoded microRNAs. J. Virol. **80:**5499–5508.
16. **Devi-Rao, G. B., D. C. Bloom, J. G. Stevens, and E. K. Wagner.** 1994. Herpes simplex virus type 1 DNA replication and gene expression during explant-induced reactivation of latently infected murine sensory ganglia. J. Virol. **68:**1271–1282.
17. **Dobson, A. T., F. Sederati, G. Devi-Rao, W. M. Flanagan, M. J. Farrell, J. G. Stevens, E. K. Wagner, and L. T. Feldman.** 1989. Identification of the latency-associated transcript promoter by expression of rabbit beta-globin mRNA in mouse sensory nerve ganglia latently infected with a recombinant herpes simplex virus. J. Virol. **63:**3844–3851.
18. **Elbashir, S. M., W. Lendeckel, and T. Tuschl.** 2001. RNA interference is mediated by 21- and 22-nucleotide RNAs. Genes Dev. **15:**188–200.

19. **Farrell, M. J., A. T. Dobson, and L. T. Feldman.** 1991. Herpes simplex virus latency-associated transcript is a stable intron. Proc. Natl. Acad. Sci. U. S. A. **88:**790–794.
20. **Friedman, R. C., K. K. Farh, C. B. Burge, and D. P. Bartel.** 2009. Most mammalian mRNAs are conserved targets of microRNAs. Genome Res. **19:**92–105.
21. **Garber, D. A., P. A. Schaffer, and D. M. Knipe.** 1997. A LAT-associated function reduces productive-cycle gene expression during acute infection of murine sensory neurons with herpes simplex virus type 1. J. Virol. **71:**5885–5893.
22. **Gregory, R. I., K. P. Yan, G. Amuthan, T. Chendrimada, B. Doratotaj, N. Cooch, and R. Shiekhattar.** 2004. The Microprocessor complex mediates the genesis of microRNAs. Nature **432:**235–240.
23. **Grimson, A., K. K. Farh, W. K. Johnston, P. Garrett-Engele, L. P. Lim, and D. P. Bartel.** 2007. MicroRNA targeting specificity in mammals: determinants beyond seed pairing. Mol. Cell **27:**91–105.
24. **Han, J., J. S. Pedersen, S. C. Kwon, C. D. Belair, Y. K. Kim, K. H. Yeom, W. Y. Yang, D. Haussler, R. Blelloch, and V. N. Kim.** 2009. Posttranscriptional crossregulation between Drosha and DGCR8. Cell **136:**75–84.
25. **Hardwicke, M. A., and P. A. Schaffer.** 1995. Cloning and characterization of herpes simplex virus type 1 oriL: comparison of replication and protein-DNA complex formation by oriL and oriS. J. Virol. **69:**1377–1388.
26. **Hardwicke, M. A., and P. A. Schaffer.** 1997. Differential effects of nerve growth factor and dexamethasone on herpes simplex virus type 1 oriL- and oriS-dependent DNA replication in PC12 cells. J. Virol. **71:**3580–3587.
27. **Hofacker, I. L.** 2003. Vienna RNA secondary structure server. Nucleic Acids Res. **31:**3429–3431.
28. **Hubenthal-Voss, J., L. Starr, and B. Roizman.** 1987. The herpes simplex virus origins of DNA synthesis in the S component are each contained in a transcribed open reading frame. J. Virol. **61:**3349–3355.
29. **Hutvagner, G., J. McLachlan, A. E. Pasquinelli, E. Balint, T. Tuschl, and P. D. Zamore.** 2001. A cellular function for the RNA-interference enzyme Dicer in the maturation of the let-7 small temporal RNA. Science **293:**834–838.
30. **Jones, C. A., T. J. Taylor, and D. M. Knipe.** 2000. Biological properties of herpes simplex virus 2 replication-defective mutant strains in a murine nasal infection model. Virology **278:**137–150.
31. **Kim, D. H., P. Saetrom, O. Snove, Jr., and J. J. Rossi.** 2008. MicroRNA-directed transcriptional gene silencing in mammalian cells. Proc. Natl. Acad. Sci. U. S. A. **105:**16230–16235.
32. **Kramer, M. F., S. H. Chen, D. M. Knipe, and D. M. Coen.** 1998. Accumulation of viral transcripts and DNA during establishment of latency by herpes simplex virus. J. Virol. **72:**1177–1185.
33. **Kramer, M. F., and D. M. Coen.** 1995. Quantification of transcripts from the ICP4 and thymidine kinase genes in mouse ganglia latently infected with herpes simplex virus. J. Virol. **69:**1389–1399.
34. **Kramer, M. F., W. J. Cook, F. P. Roth, J. Zhu, H. Holman, D. M. Knipe, and D. M. Coen.** 2003. Latent herpes simplex virus infection of sensory neurons alters neuronal gene expression. J. Virol. **77:**9533–9541.
35. **Kruger, J., and M. Rehmsmeier.** 2006. RNAhybrid: microRNA target prediction easy, fast and flexible. Nucleic Acids Res. **34:**W451–W454.
36. **Langenberger, D., C. Bermudez-Santana, J. Hertel, S. Hoffmann, P. Khaitovich, and P. F. Stadler.** 2009. Evidence for human microRNA-offset RNAs in small RNA sequencing data. Bioinformatics **25:**2298–2301.
37. **Larkin, M. A., G. Blackshields, N. P. Brown, R. Chenna, P. A. McGettigan, H. McWilliam, F. Valentin, I. M. Wallace, A. Wilm, R. Lopez, J. D. Thompson, T. J. Gibson, and D. G. Higgins.** 2007. Clustal W and Clustal X version 2.0. Bioinformatics **23:**2947–2948.
38. **Lau, N. C., L. P. Lim, E. G. Weinstein, and D. P. Bartel.** 2001. An abundant class of tiny RNAs with probable regulatory roles in Caenorhabditis elegans. Science **294:**858–862.
39. **Lee, Y., C. Ahn, J. Han, H. Choi, J. Kim, J. Yim, J. Lee, P. Provost, O. Radmark, S. Kim, and V. N. Kim.** 2003. The nuclear RNase III Drosha initiates microRNA processing. Nature **425:**415–419.
40. **Lee, Y., K. Jeon, J. T. Lee, S. Kim, and V. N. Kim.** 2002. MicroRNA maturation: stepwise processing and subcellular localization. EMBO J. **21:**4663–4670.
41. **Lewis, B. P., C. B. Burge, and D. P. Bartel.** 2005. Conserved seed pairing, often flanked by adenosines, indicates that thousands of human genes are microRNA targets. Cell **120:**15–20.
42. **Lewis, B. P., I. H. Shih, M. W. Jones-Rhoades, D. P. Bartel, and C. B. Burge.** 2003. Prediction of mammalian microRNA targets. Cell **115:**787–798.
43. **Li, R., Y. Li, K. Kristiansen, and J. Wang.** 2008. SOAP: short oligonucleotide alignment program. Bioinformatics **24:**713–714.
44. **Liu, J., M. A. Carmell, F. V. Rivas, C. G. Marsden, J. M. Thomson, J. J. Song, S. M. Hammond, L. Joshua-Tor, and G. J. Hannon.** 2004. Argonaute2 is the catalytic engine of mammalian RNAi. Science **305:**1437–1441.
45. **Liu, J., F. V. Rivas, J. Wohlschlegel, J. R. Yates III, R. Parker, and G. J. Hannon.** 2005. A role for the P-body component GW182 in microRNA function. Nat. Cell Biol. **7:**1261–1266.
46. **McGeoch, D. J., C. Cunningham, G. McIntyre, and A. Dolan.** 1991. Comparative sequence analysis of the long repeat regions and adjoining parts of the long unique regions in the genomes of herpes simplex viruses types 1 and 2. J. Gen. Virol. **72:**3057–3075.
47. **Perng, G. C., C. Jones, J. Ciacci-Zanella, M. Stone, G. Henderson, A. Yukht, S. M. Slanina, F. M. Hofman, H. Ghiasi, A. B. Nesburn, and S. L. Wechsler.** 2000. Virus-induced neuronal apoptosis blocked by the herpes simplex virus latency-associated transcript. Science **287:**1500–1503.
48. **Pesola, J. M., J. Zhu, D. M. Knipe, and D. M. Coen.** 2005. Herpes simplex virus 1 immediate-early and early gene expression during reactivation from latency under conditions that prevent infectious virus production. J. Virol. **79:**14516–14525.
49. **Pfeffer, S., A. Sewer, M. Lagos-Quintana, R. Sheridan, C. Sander, F. A. Grasser, L. F. van Dyk, C. K. Ho, S. Shuman, M. Chien, J. J. Russo, J. Ju, G. Randall, B. D. Lindenbach, C. M. Rice, V. Simon, D. D. Ho, M. Zavolan, and T. Tuschl.** 2005. Identification of microRNAs of the herpesvirus family. Nat. Methods **2:**269–276.
50. **Rehmsmeier, M., P. Steffen, M. Hochsmann, and R. Giegerich.** 2004. Fast and effective prediction of microRNA/target duplexes. RNA **10:**1507–1517.
51. **Roizman, B., D. M. Knipe, and R. J. Whitley.** 2007. Herpes simplex viruses, p. 2501–2602. *In* D. M. Knipe and P. M. Howley (ed.), Fields virology, 5th ed., vol. 2. Lippincott, Williams & Wilkins, New York, NY.
52. **Ruby, J. G., A. Stark, W. K. Johnston, M. Kellis, D. P. Bartel, and E. C. Lai.** 2007. Evolution, biogenesis, expression, and target predictions of a substantially expanded set of Drosophila microRNAs. Genome Res. **17:**1850–1864.
53. **Schwarz, D. S., G. Hutvagner, T. Du, Z. Xu, N. Aronin, and P. D. Zamore.** 2003. Asymmetry in the assembly of the RNAi enzyme complex. Cell **115:**199–208.
54. **Shi, W., D. Hendrix, M. Levine, and B. Haley.** 2009. A distinct class of small RNAs arises from pre-miRNA-proximal regions in a simple chordate. Nat. Struct. Mol. Biol. **16:**183–189.
55. **Stevens, J. G., E. K. Wagner, G. B. Devi-Rao, M. L. Cook, and L. T. Feldman.** 1987. RNA complementary to a herpesvirus alpha gene mRNA is prominent in latently infected neurons. Science **235:**1056–1059.
56. **Tal-Singer, R., T. M. Lasner, W. Podrzucki, A. Skokotas, J. J. Leary, S. L. Berger, and N. W. Fraser.** 1997. Gene expression during reactivation of herpes simplex virus type 1 from latency in the peripheral nervous system is different from that during lytic infection of tissue cultures. J. Virol. **71:**5268–5276.
57. **Tang, S., A. S. Bertke, A. Patel, K. Wang, J. I. Cohen, and P. R. Krause.** 2008. An acutely and latently expressed herpes simplex virus 2 viral microRNA inhibits expression of ICP34.5, a viral neurovirulence factor. Proc. Natl. Acad. Sci. U. S. A. **105:**10931–10936.
58. **Tang, S., A. Patel, and P. R. Krause.** 2009. Novel less-abundant viral microRNAs encoded by herpes simplex virus 2 latency-associated transcript and their roles in regulating ICP34.5 and ICP0 mRNAs. J. Virol. **83:**1433–1442.
59. **Thompson, R. L., and N. M. Sawtell.** 2001. Herpes simplex virus type 1 latency-associated transcript gene promotes neuronal survival. J. Virol. **75:**6660–6675.
60. **Triboulet, R., H. M. Chang, R. J. Lapierre, and R. I. Gregory.** 2009. Post-transcriptional control of DGCR8 expression by the Microprocessor. RNA **15:**1005–1011.
61. **Tyler, D. M., K. Okamura, W. J. Chung, J. W. Hagen, E. Berezikov, G. J. Hannon, and E. C. Lai.** 2008. Functionally distinct regulatory RNAs generated by bidirectional transcription and processing of microRNA loci. Genes Dev. **22:**26–36.
62. **Umbach, J. L., and B. R. Cullen.** 2010. In-depth analysis of Kaposi's sarcoma-associated herpesvirus microRNA expression provides insights into the mammalian microRNA-processing machinery. J. Virol. **84:**695–703.
63. **Umbach, J. L., and B. R. Cullen.** 2009. The role of RNAi and microRNAs in animal virus replication and antiviral immunity. Genes Dev. **23:**1151–1164.
64. **Umbach, J. L., M. F. Kramer, I. Jurak, H. W. Karnowski, D. M. Coen, and B. R. Cullen.** 2008. MicroRNAs expressed by herpes simplex virus 1 during latent infection regulate viral mRNAs. Nature **454:**780–783.
65. **Umbach, J. L., M. A. Nagel, R. J. Cohrs, D. H. Gilden, and B. R. Cullen.** 2009. Analysis of human alphaherpesvirus microRNA expression in latently infected human trigeminal ganglia. J. Virol. **83:**10677–10683.
66. **Umbach, J. L., K. Wang, S. Tang, P. R. Krause, E. K. Mont, J. I. Cohen, and B. R. Cullen.** 2010. Identification of viral microRNAs expressed in human sacral ganglia latently infected with herpes simplex virus 2. J. Virol. **84:**1189–1192.
67. **Wang, Q. Y., C. Zhou, K. E. Johnson, R. C. Colgrove, D. M. Coen, and D. M. Knipe.** 2005. Herpesviral latency-associated transcript gene promotes assembly of heterochromatin on viral lytic-gene promoters in latent infection. Proc. Natl. Acad. Sci. U. S. A. **102:**16055–16059.
68. **Yager, D. R., and D. M. Coen.** 1988. Analysis of the transcript of the herpes simplex virus DNA polymerase gene provides evidence that polymerase expression is inefficient at the level of translation. J. Virol. **62:**2007–2015.
69. **Zuker, M.** 2003. Mfold web server for nucleic acid folding and hybridization prediction. Nucleic Acids Res. **31:**3406–3415.